Talanta 116 (2013) 794–800

Contents lists available at ScienceDirect

Talanta

journal homepage: www.elsevier.com/locate/talanta

Phosphorescence detection of L-ascorbic acid with surface-attached *N*-acetyl-L-cysteine and L-cysteine Mn doped ZnS quantum dots

Wei Bian [a,b], Jing Ma [b], Wenrong Guo [b], Dongtao Lu [a], Meng Fan [a], Yanli Wei [a], Yingfu Li [a], Shaomin Shuang [a,*], Martin M.F. Choi [c,**]

[a] School of Chemistry and Chemical Engineering, Shanxi University, Taiyuan 030006, PR China
[b] School of Basic Medical Science, Shanxi Medical University, Taiyuan 030001, PR China
[c] Department of Chemistry, Hong Kong Baptist University, 224 Waterloo Road, Kowloon Tong, Hong Kong SAR, PR China

ARTICLE INFO

Article history:
Received 26 April 2013
Received in revised form
24 July 2013
Accepted 27 July 2013
Available online 7 August 2013

Keywords:
Mn doped ZnS quantum dots
Phosphorescence probe
L-Ascorbic acid

ABSTRACT

N-Acetyl-L-cysteine (NAC) and L-cysteine (Cys) capped Mn doped ZnS quantum dots (NAC-Mn/ZnS QDs and Cys-Mn/ZnS QDs) are firstly prepared by hydrothermal methods. These QDs display strong phosphorescence emission peaks at 583 and 580 nm upon excitation at 315 and 306 nm, respectively. Since their room-temperature phosphorescence is efficiently quenched by L-ascorbic acid (AA), they have been employed as phosphorescence probes for detecting AA. The linear working ranges are 2.5–37.5 and 2.5–47.5 μM and the limits of detection are 0.72 and 1.38 μM for NAC-Mn/ZnS QDs and Cys-Mn/ZnS QDs, respectively. The possible quenching mechanisms have been discussed in detail. The QDs probes are highly selective to AA over other common ions, amino acids, glucose and bovine serum album. Finally, they have been applied successfully for detection of AA in human urine samples with satisfactory results. The recoveries are 98–104%. Our work provides a simple and convenient phosphorescence method to determine AA in real samples.

1. Introduction

L-Ascorbic acid (AA) is usually found in body fluids at relatively high concentrations as a vital antioxidant and plays an important role in balancing the oxidative stress of human body. It also takes part in a lot of biochemical processes, *e.g.*, as an enzymatic cofactor for the synthesis of carnitine, catecholamine and myelin [1,2]. In addition, AA serves as a medication for scurvy, allergic reactions and atherosclerosis, and helps promote healthy cell development, calcium absorption and normal tissue growth in the clinic [3]. However, excessive intake of AA can result in diarrhea, hyperacidity and kidney calculi [4].

So far numerous analytical techniques for the determination of AA including UV–vis absorption spectrophotometry [5], spectrofluorometry [6], enzymatic analysis [7], electroanalysis [8], colorimetry [9–11], chemiluminescence [12] and high-performance liquid chromatography (HPLC) [13] have been proposed. But these methods, to certain extent, suffer from some complicated extraction procedures, expensive cost and long operation time. As such, efforts have been continued to spend in order to improve the simplicity, sensitivity, selectivity and utility in pharmaceutical industry and clinical analysis [14].

Colloidal semiconductor nanocrystals as quantum dots (QDs) benefit from many unique properties such as high luminescence efficiency, wide and continuous excitation spectrum, narrow and symmetric emission spectrum, adjustable color, and good photochemical stability. Moreover, these QDs offer the possible application in fluorescent sensing. The direct interaction between certain analytes and the surface of QDs can influence the efficiency of the electron–hole recombination process [15]. Thus, QDs have been widely applied to detect different kinds of analytes including ions [16], small molecules [17], and biological macromolecule [18,19]. Most of the detection methods are relied on the fluorescence properties of these QDs. To our knowledge, there is not much work on making use of the inherent phosphorescence properties of QDs.

Room-temperature phosphorescence (RTP) as a powerful tool for optical sensing has increasingly attracted much attention since it affords many advantages over fluorescence. The triplet excited state of phosphorescence provides several virtues, for instance, longer emission lifetime, wider gap between the excitation and emission wavelengths, and minimum interference from the short-lived auto-fluorescence and scattering light [20,21]. At the same time, selectivity of detection can be improved because phosphorescence is a less usual phenomenon than that of fluorescence [22]. It is well known that doped semiconductor nanocrystals, replacing

* Corresponding author. Tel.: +86 351 7018842; fax: +86 351 7011322.
** Corresponding author. Tel.: +852 34117839; fax: +852 34117348.
E-mail addresses: smshuang@sxu.edu.cn (S. Shuang), mfchoi@hkbu.edu.hk (M.M.F. Choi).

0039-9140/$ - see front matter © 2013 Elsevier B.V. All rights reserved.
http://dx.doi.org/10.1016/j.talanta.2013.07.076

the cadmium in cadmium chalcogenide QDs with zinc as the absorption zone and importing the transition metals (Mn or Cu) as the emissive center [23], cannot only retain most of the outstanding properties of QDs, but also alleviate the toxicity puzzles. Especially, impurities introduced intentionally can strongly modify the optical properties of bulk semiconductors [24]. Yan et al. has demonstrated that RTP of doped ZnS QDs can be applied to determine DNA, persistent organic pollutants in water, glucose, enoxacin and other drugs in biological fluids [25–29]. Wu and Fan also found that doped ZnS QDs can act as phosphorescence sensors for detecting raceanisodamie hydrochloride and atropine sulfate in biological fluids [30]. It is postulated that the construction of hybrid QDs as the phosphorescence sensing platform is desirable and viable.

In the present study, water-soluble Mn doped ZnS QDs surface-capped with *N*-acetyl-L-cysteine (NAC) and L-cysteine (Cys) are firstly synthesized by a hydrothermal method. Since NAC and Cys are nontoxic and possess good water-solubility, the as-synthesized NAC-Mn/ZnS QDs and Cys-Mn/ZnS QDs could be potentially useful for RTP detection of water-soluble analytes in biological samples. It was found that the RTP of NAC-Mn/ZnS QDs and Cys-Mn/ZnS QDs were efficiently quenched by AA. In this work, these QDs have been successfully applied to determine the AA content in human urine samples with satisfactory results. The quenching mechanism has been studied by time-resolved spectroscopy. Our work demonstrates that the as-synthesized NAC-Mn/ZnS QDs and Cys-Mn/ZnS QDs probes show potential in biomedical or clinical analysis via RTP.

2. Experimental

2.1. Chemicals and reagents

N-acetyl-L-cysteine and L-cysteine were purchased from Aladdin Chemicals (Leonard, TX, USA). $ZnSO_4 \cdot 7H_2O$, $MnCl_2 \cdot 4H_2O$ and $Na_2S \cdot 9H_2O$ were obtained from Tianjin Chemical Reagent Company (Tianjin, China). L-Ascorbic acid was from Shanghai Reagent Factory (Shanghai, China). Other analytical grade reagents were purchased from Beijing Chemical Reagent Company (Beijing, China). Purified water from a Milli-Q-RO_4 water purification system (Millipore, Bedford, MA, USA) with a resistivity higher than 18 MΩ/cm was used to prepare all solutions. All chemicals of analytical reagent grade or above were used as received. 50 mM Phosphate buffer solutions (PBS) were prepared by mixing appropriate volumes of standard solutions of 50 mM Na_2HPO_4 and 50 mM NaH_2PO_4. The buffers were adjusted to required pH with 50 mM H_3PO_4 or 1.0 M NaOH solutions.

2.2. Synthesis of Mn doped ZnS QDs

N-Acetyl-L-cysteine capped Mn doped ZnS QDs were synthesized in aqueous solution according to a literature method with minor modifications [31]. Briefly, to a three-necked flask, aqueous solutions of $ZnSO_4 \cdot 7H_2O$, $MnCl_2 \cdot 4H_2O$ and NAC were added and the final volume of the mixture was 50 mL. The pH of the solution was adjusted to 11 with 1.0 M NaOH. After removal of air with nitrogen bubbling at room temperature, an aqueous solution of $Na_2S \cdot 9H_2O$ was quickly injected into the reaction mixture and stirred. Then the mixture was aged for 2.5 h to obtain the NAC-Mn/ZnS QDs product. After purification and centrifugation, the as-synthesized NAC-Mn/ZnS QDs were dried in vacuum. The QDs product is very water-soluble. Similarly, Cys-Mn/ZnS QDs were synthesized. (Scheme 1)

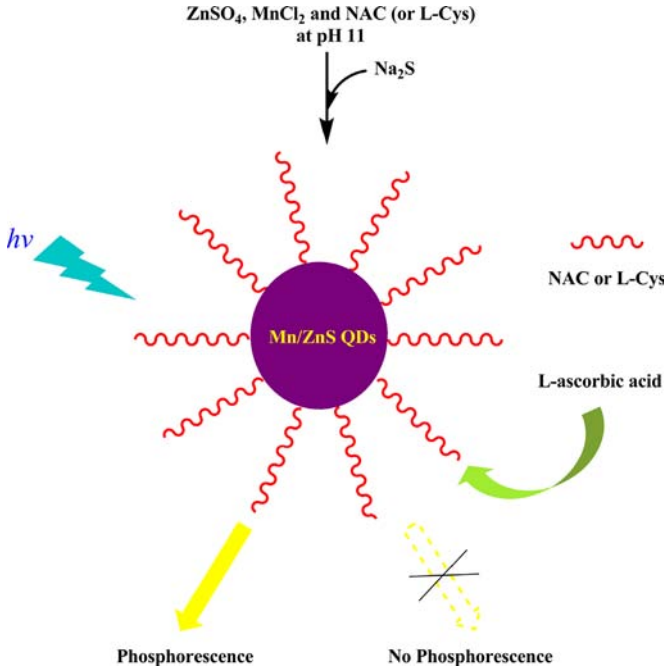

Scheme 1. Schematic illustration of the sensor design.

2.3. Instrumentation

The absorption and fluorescence measurements were carried out on a Shimadzu UV-265 absorption spectrophotomter (Tokyo, Japan) and a Hitachi F-4500 spectrofluorometer (Tokyo, Japan), respectively. Excitation and emission bandwidths were both set at 10 nm. A 150 W xenon arc lamp was used as the excitation light source. A standard 1.0 cm quartz cell was used. pH measurements were taken on a Model pHS-3C pH-meter (Shanghai Rex Instrument Factory, Shanghai, China). Phosphorescence lifetime measurements were performed on an Edinburgh FLS920 spectrometer (Edinburgh, UK). A microsecond pulsed xenon flash lamp was used as the excitation light source in the determination of RTP lifetime. Transmission electron microscopic (TEM) images of QDs were obtained with a JEOL JEM-1011 transmission electron microscopy (Tokyo, Japan) operating at 200 kV. Samples were prepared by casting and evaporating a droplet of aqueous solution of QDs onto Agar Scientific 400 mesh copper grids (Essex, UK). Fourier transform infrared (FT-IR) spectra of QDs and free ligands were performed on a Perkin-Elmer Paragon 1000 FTIR spectrometer (Waltham, MA, USA) with the KBr pellet technique ranging 500–4000 cm^{-1}. All experiments were performed at 20 ± 1 °C.

2.4. Phosphorescence measurement

4.5 mL of 50 mg L^{-1} Mn/ZnS QDs solution, 5.0 mL of PBS (pH 8.0) and various concentrations of AA standard or urine sample were introduced into a 10 mL calibrated test tube. Then the mixture was diluted to the volume with high-purity water and mixed thoroughly. The tube was stood for 10 min and a portion of the solution was transferred into a 10-mm silica cuvette for phosphorescence measurement.

4.5 mL of 50 mg L^{-1} Mn/ZnS QDs solution, 5.0 mL of PBS (pH 8.0), 50 μL of 0.10 mM AA standard and 50 μL of different concentrations of interfering components were introduced into a 10 mL calibrated test tube. Then the mixture was diluted to the volume with high-purity water and mixed thoroughly. The tube was stood for 10 min and a portion of the solution was transferred into a 10-mm silica cuvette for phosphorescence measurement. RTP was taken at an

excitation wavelength of 306 or 315 nm with excitation and emission slit widths of 10 nm.

The urine samples were collected from healthy volunteers. The samples were diluted 1000-fold with water before analysis. No sample pretreatments such as deproteinization or centrifugation were required. The determinations of AA in urine samples were also conducted by a reference method [5]. The results obtained were compared with that of our proposed RTP method.

3. Results and discussion

3.1. Characterization of Mn/ZnS QDs

The morphologies of NAC-Mn/ZnS and Cys-Mn/ZnS QDs were assessed by TEM as depicted in Fig. S1 (Supplementary Data). Both NAC-Mn/ZnS and Cys-Mn/ZnS QDs display nearly spherical shape and have average diameters of *ca.* 8–10 nm. The QDs tend to cluster together under TEM since they are prepared in dry state. Various spectroscopic techniques were also employed for characterization of the Mn/ZnS QDs. Fig. S2 depicts the FT-IR spectra of the NAC-Mn/ZnS QDs, Cys-Mn/ZnS QDs and the free ligands NAC and Cys. The absorption band at 2570 cm^{-1} corresponding to sulfhydryl group disappears in the NAC-Mn/ZnS QDs spectrum. The stretching vibration band of the carboxyl group at 1710 cm^{-1} of NAC is shifted to 1590 cm^{-1} after binding to QDs. These results indicate that NAC has successfully capped on the surface of Mn/ZnS QDs by the sulfhydryl functionality. Similarly, the S–H vibration band of Cys at 2600 cm^{-1} is vanished after it has linked to the Mn/ZnS QDs. The absorption bands at *ca.* 1400 (m_s COO^-), 1550–1600 (s_s COO^-), and 3500–3000 cm^{-1} (m_s OH, COOH) corresponding to the carboxylic functionality and 2900–3420 cm^{-1} attributing to the amino group are observed in the Cys-Mn/ZnS QDs spectrum, indicating that Cys has been attached to the surface of Mn/ZnS QDs.

The as-synthesized NAC-Mn/ZnS QDs and Cys-Mn/ZnS QDs could disperse well in aqueous solution. The phosphorescence intensity is stable. No significant changes in their RTP or noticeable aggregation were observed over several weeks when the QDs were kept in dark under ambient conditions. The phosphorescence spectra are easy to acquire without the use of deoxidant or inducers and is thus superior to the traditional phosphorescence measurement. Fig. S3A depicts the phosphorescence excitation and emission spectra of NAC-Mn/ZnS QDs with excitation and emission maxima of 315 nm and 583 nm, respectively. Fig. S3B displays the phosphorescence excitation and emission spectra of Cys-Mn/ZnS QDs. The excitation and emission maxima are at 306 and 580 nm, respectively. There is not much difference between the phosphorescence spectra of NAC-Mn/ZnS and Cys-Mn/ZnS QDs. The phosphorescence emission at 580–583 nm corresponds to the $^4T_1$ (the triplet state)–$^6A_1$ (the ground state) transition of Mn^{2+} impurity, indicating Mn^{2+} has entered into the ZnS lattice to form Mn doped ZnS QDs [32]. The photoluminescence quantum yields of NAC-Mn/ZnS and Cys-Mn/ZnS QDs were determined as 4.8 and 4.0%, respectively, using rhodamine 6G as the reference.

3.2. Optimization of detection of L-ascorbic acid

3.2.1. pH and buffer

The effect of pH (4.0–10.5) on the phosphorescence intensity of Mn/ZnS QDs in the presence of AA was examined. Several buffer systems such as Tris–HCl, PBS and Bristton–Robinson buffer were tested. It was observed that Mn/ZnS QDs were most remarkably quenched by AA in the PBS system. Thus, PBS was selected as the optimum buffer solution. Fig. 1 displays the plots of (P_0–P) against pH, where P_0 and P are the phosphorescence intensity of Mn/ZnS QDs in the absence and presence of AA. The phosphorescence intensity is quenched by AA. The quenching effect (P_0–P) increases dramatically with the increase in pH from 4.0 to 8.0 and decreases with further in pH. As such, 8.0 was chosen as the optimal pH for AA determination since it produces the highest quenching effect.

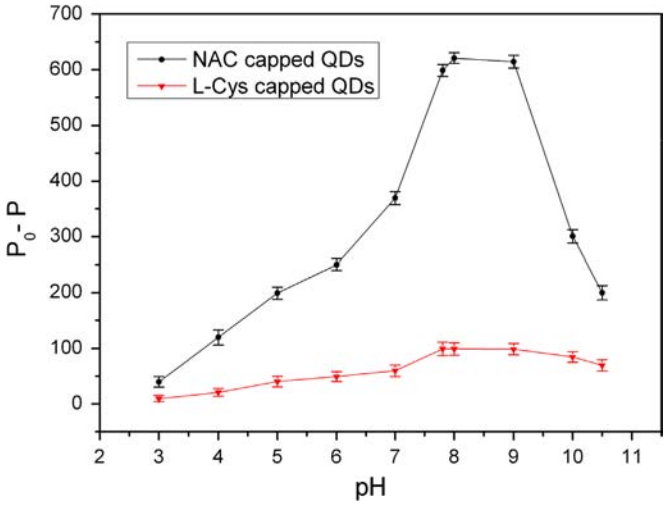

Fig. 1. Effect of pH on the phosphorescence intensity of NAC-Mn/ZnS QDs and Cys-Mn/ZnS QDs with and without L-ascorbic acid. Plot of P_0–P against pH, where P_0 and P are the phosphorescence intensity in the absence and presence of L-ascorbic acid. The concentrations of QDs and L-ascorbic acid are 22.5 mg/L and 25 μM, respectively.

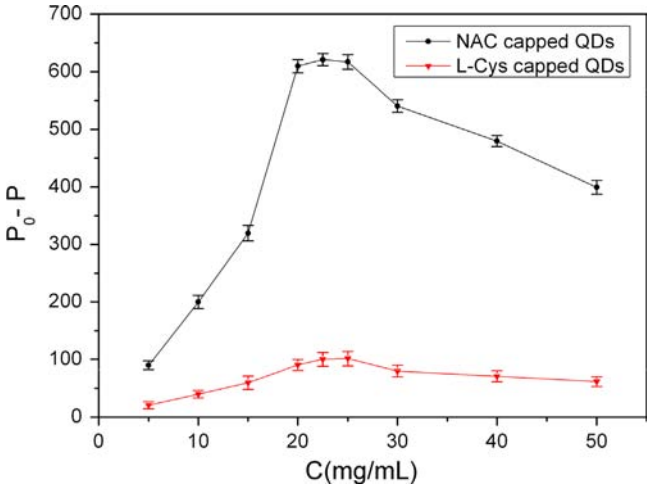

Fig. 2. Effect of concentration (C) of NAC-Mn/ZnS QDs and Cys-Mn/ZnS QDs in PBS (pH 8.0) on phosphorescence quenching by L-ascorbic acid. Plot of (P_0–P) against C, where P_0 and P are the phosphorescence intensity in the absence and presence of 25 μM L-ascorbic acid, respectively.

3.2.2. Concentration of Mn/ZnS QDs and reaction time

Fig. 2 shows the effect of QDs concentration on the phosphorescence quenching by AA. The phosphorescence intensity is quenched by AA. The quenching effect increases with the increase in the concentration of QDs until it reaches the highest at 22.5 mg/L. Further increase in QDs concentration would cause a decrease in the quenching. When the concentration of QDs is too low, the phosphorescence intensity will be very weak, resulting in noisy and unstable signal. By contrast, if the concentration of QDs is too high, the quenching effect is lower attributing to the self-quenching of the QDs. Thus, 22.5 mg/L of QDs is chosen for the subsequent work.

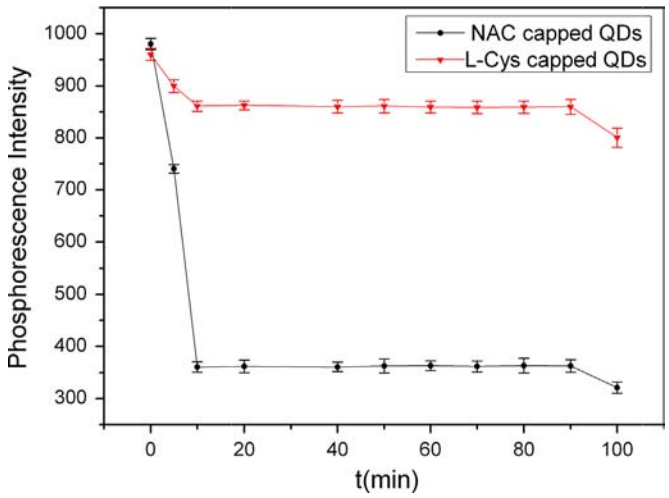

Fig. 3. Effect of reaction time on the phosphorescence quenching of 22.5 mg/mL NAC-Mn/ZnS QDs and Cys-Mn/ZnS QDs in PBS (pH 8.0) with 25 μM L-ascorbic acid.

Fig. 3 displays the effect of reaction time on the phosphorescence intensity of 22.5 mg/mL Mn/ZnS QDs with 25 μM AA in PBS (pH 8.0). The intensity drops significantly in the first 10 min and reaches the lowest at 10 min. The intensity remains more or less the same for at least 1.5 h. Thus, 10 min is chosen the optimal reaction time between Mn/ZnS QDs and AA.

3.3. Phosphorescence quenching of Mn/ZnS QDs by L-ascorbic acid

The effect of various concentrations of AA on the phosphorescence of Mn/ZnS QDs was studied. Fig. 4 depicts the emission spectra of (A) NAC-Mn/ZnS QDs and (B) Cys-Mn/ZnS QDs at different concentrations of AA. The intensities decrease with the increase in the concentration of AA and there is no discernible change in the spectral characteristics of Mn/ZnS QDs, indicating the dynamic quenching of AA on Mn/ZnS QDs. The insets display the Stern–Volmer plots of P_0/P against concentration of L-ascorbic acid where P_0 and P are the intensities in the absence and presence of AA, respectively. The curves show linear ranges of 2.5–37.5 and 2.5–47.5 μM AA with correlation coefficients of 0.9983 and 0.9950 for (A) NAC-Mn/ZnS QDs and (B) Cys-Mn/ZnS QDs, respectively. The linear regression equations are $P_0-P=58.366$ [AA]+22.703 and $P_0-P=39.078$ [AA]+12.214 for NAC-Mn/ZnS QDs and Cys-Mn/ZnS QDs, respectively. AA shows stronger quenching effect on NAC-Mn/ZnS QDs than that of Cys-Mn/ZnS QDs. The relative standard deviations (RSDs) for 11 replicate detections of AA (10 μM) are 1.4 and 1.8% based on NAC-Mn/ZnS QDs and Cys-Mn/ZnS QDs, respectively. The limits of detection (LODs) are 0.72 and 13.8 μM AA for NAC-Mn/ZnS QDs and Cys-Mn/ZnS QDs, respectively. The results indicate that NAC-Mn/ZnS QDs has higher sensitivity and lower LOD than that of Cys-Mn/ZnS QDs for detection of AA.

3.4. Quenching mechanism

The photoluminescence response mechanism of Mn/ZnS QDs originates from the recombination of electron–hole pair upon excitation. Once the radiative recombination is suppressed, photoluminescence quenching is usually observed. This phenomenon could be attributed to interactions of molecules or ions with the surface atoms of QDs [33,34]. Phosphorescence quenching is usually divided into static and dynamic quenching. Static quenching takes place between the quencher and phosphorescence substance in the ground state, thus generating lightless complexes with a concomitant decrease in phosphorescence intensity. However, the

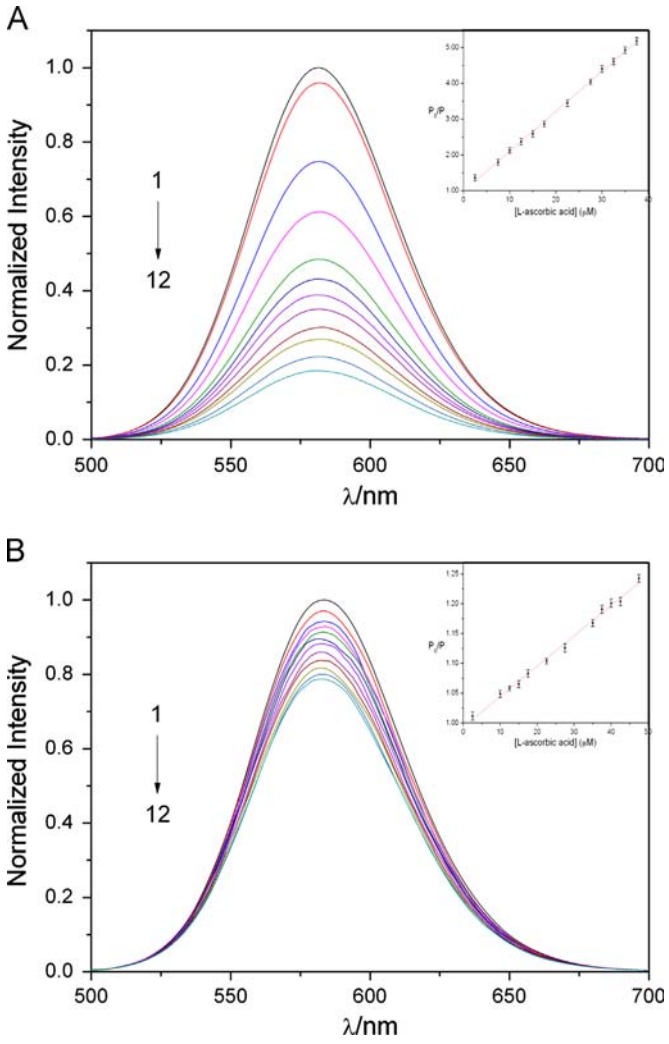

Fig. 4. Phosphorescence intensity of (A) NAC-Mn/ZnS QDs at various concentrations of L-ascorbic acid: (1) 0.0, (2) 2.5, (3) 5.0, (4) 7.5, (5) 10.0, (6) 12.5, (7) 15.0, (8) 17.5, (9) 22.5, (10) 27.5, (11) 35.2, and (12) 37.5 μM. (B) Cys-Mn/ZnS QDs at various concentrations of L-ascorbic acid: (1) 0.0, (2) 2.5, (3) 7.5, (4) 12.5, (5) 22.5, (6) 27.5, (7) 30.0, (8) 32.5, (9) 37.5, (10) 35.0, (11) 42.5, and (12) 47.5 μM. The insets display the Stern–Volmer plots of P_0/P against concentration of L-ascorbic acid where P_0 and P are the intensities in the absence and presence of L-ascorbic acid, respectively. The excitation/emission wavelengths are monitored at 315/583 and 306/580 nm for NAC-Mn/ZnS and Cys-Mn/ZnS QDs in pH 8.0 PBS, respectively.

lifetime of RTP remains unchanged under static quenching condition. For dynamic quenching, the interaction is taken place between the quencher and excited state of the phosphorescence material, resulting in the decrease in intensity and lifetime of the phosphorescence molecule. The dynamic process could be described by Stern–Volmer relationship as: $P_0/P=1+K_{SV}$[AA] or $\tau_0/\tau=1+k_q\tau_0$[AA], where P_0 and P, and τ_0 and τ are the phosphorescence intensities and lifetimes of Mn/ZnS QDs in the absence and in the presence of AA, respectively, [AA] is the concentration of the AA, K_{SV} is the Stern–Volmer quenching constant, and k_q is the bimolecular quenching rate constant. The insets of Fig. 4 show the Stern–Volmer plots using P_0/P against [AA] based on NAC-Mn/ZnS and Cys-Mn/ZnS QDs, respectively. Both curves display good linear relationship in the range 2.5–37.5 and 2.5–47.5 μM AA and the K_{SV} are determined as 9.3×10^4 and 5.12×10^3 M^{-1}, respectively. In addition, the phosphorescence decays were also utilized to confirm the quenching mechanism of AA on Mn/ZnS QDs. The decay of Mn/ZnS QDs in the absence of AA could be fitted by a biexponential function as: $I_{lum}=A_1\times e^{-(t/\tau_1)}+A_2\times e^{-(t/\tau_2)}$, where I_{lum} is the photoluminescence

intensity, τ_1 and τ_2 are the time constants of fast and slow decays, respectively, and A_1 and A_2 are the weights of each time constant. The τ_1 and τ_2 of NAC-Mn/ZnS QDs are determined to be 1.09 and 4.69 ms with relative weights of 24.7 and 75.3%, respectively. For Cys-Mn/ZnS QDs, the τ_1 and τ_2 are 1.05 and 4.47 ms with relative weights of 19.9 and 80.1%, respectively. The lifetimes of NAC-Mn/ZnS and Cys-Mn/ZnS QDs are long and very close with each other. Both τ_1 and τ_2 decrease with the increase in the concentration of AA. The insets of Fig. 5 display the plot of τ_{01}/τ_1 and τ_{02}/τ_2 versus L-ascorbic acid concentration for NAC-Mn/ZnS and Cys-Mn/ZnS QDs where τ_{01} and τ_{02}, and τ_1 and τ_2 are time constant 1 and 2 in the absence and presence of AA, respectively. The plots exhibit good linear relationships between τ_{01}/τ_1 or τ_{02}/τ_2 and [AA], indicating that the dynamic quenching dominates the reaction. k_q of NAC-Mn/ZnS QDs are 4.75×10^7 and $9.6\times10^6\ M^{-1}\ s^{-1}$ for time constant 1 and 2, respectively. k_q of Cys-Mn/ZnS QDs are $3.04\times10^7\ M^{-1}\ s^{-1}$ and $7.5\times10^6\ M^{-1}\ s^{-1}$ for time constant 1 and 2, respectively. The bimolecular quenching rate constants of NAC-Mn/ZnS QDs are higher than that of Cys-Mn/ZnS QDs, inferring that NAC-Mn/ZnS QDs is better quenched by AA.

The detection of AA by Mn/ZnS QDs can be described by the following mechanisms. The electron of Mn/ZnS QDs in its valence band promotes to the conduction band upon photo-excitation, resulting in the production of a positively charged hole in its valence band and a free electron in its conduction band of Mn/ZnS QDs. The phosphorescence emission of Mn/ZnS QDs derived from the triple transition of Mn^{2+} ($^4T_1$–$^6A_1$) is incorporated into the ZnS host lattice. The excitation of Mn^{2+} occurs by energy transfer from the ZnS host with a concomitant generation of the electron–hole pair. In essence, Mn^{2+} traps a hole to form Mn^{3+} (Step 1). The recombination of Mn^{3+} with an electron leads to produce the excited state of Mn^{2+} (Step 2) with subsequent phosphorescence emission (Step 3) as depicted in Fig. 6. Any factors influencing step 1 – 3 would alter the phosphorescence emission of Mn/ZnS QDs [35–38]. For instance, the direct oxidation of catecholamine results in the quenching of the photoluminescence of nanoparticles. The hydroxyl groups of catechol are traps of the holes, which could prevent the recombination of electron and hole, and thus quench the photoluminescence of nanocrystals [39]. In a similar analogy, the quenching of Mn/ZnS QDs by AA can be explained by the oxidation of AA to dehydro-AA with Mn^{3+}, inhibiting the electron–hole recombination at the interfaces of

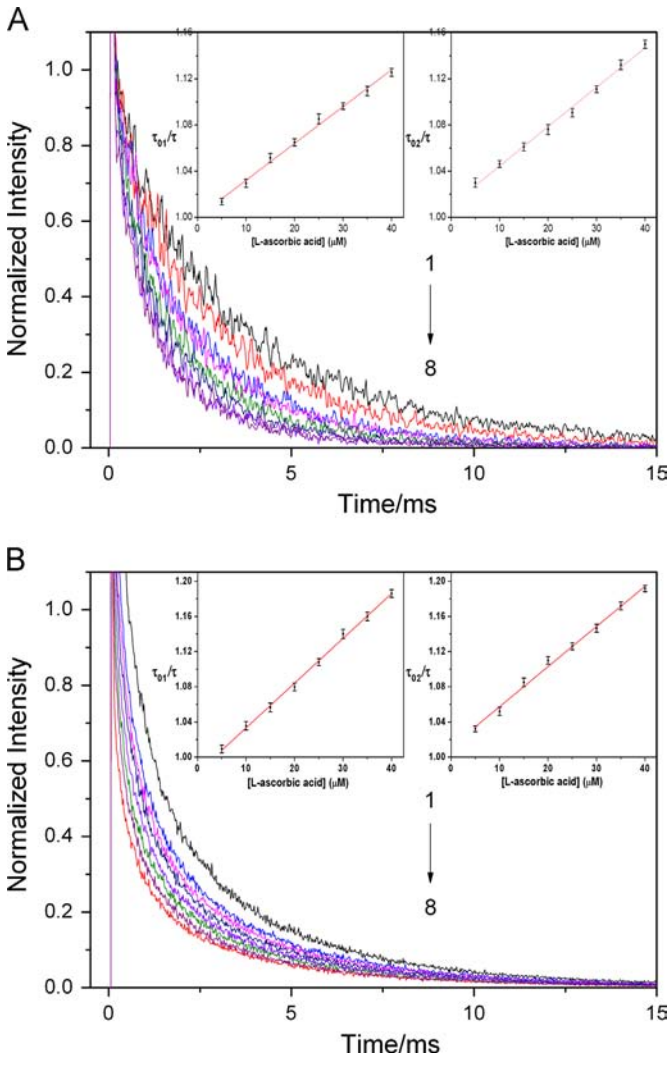

Fig. 5. Time-resolved spectra of (A) NAC-Mn/ZnS at various concentrations of L-ascorbic acid (1) 0.0, (2) 5.0, (3) 10.0, (4) 15.0, (5) 20.0, (6) 25.0, (7) 30.0, and (8) 35.0 μM. (B) Cys-Mn/ZnS QDs at various concentrations of L-ascorbic acid: (1) 0.0, (2) 5.0, (3) 10.0, (4) 15.0, (5) 20.0, (6) 25.0, (7) 30.0, and (8) 35.0 μM. The insets depict the plots of τ_{01}/τ_1 and τ_{02}/τ_2 against concentration of L-ascorbic acid where τ_{01} and τ_{02}, and τ_1 and τ_2 are the time constant 1 and 2 in the absence and presence of L-ascorbic acid, respectively. The intensities are monitored at excitation/emission wavelengths of 315/583 and 306/580 nm for NAC-Mn/ZnS and Cys-Mn/ZnS QDs in pH 8.0 PBS, respectively.

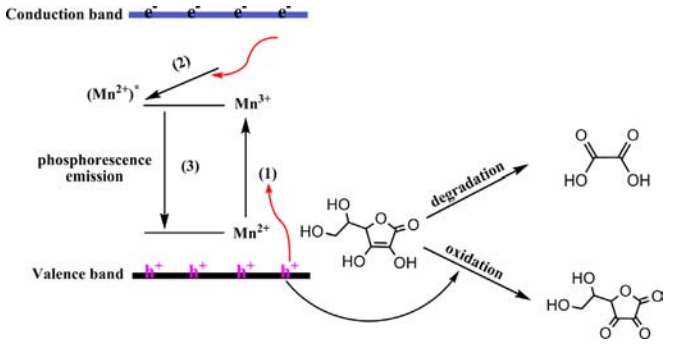

Fig. 6. Schematic illustration of the mechanism of NAC-Mn/ZnS phosphorescence quenching in the presence of L-ascorbic acid.

Table 1
Effect of potential interferents on the RTP quenching of Mn/ZnS QDs.

Type of QDs	Interferents	Ratio of concentration of interferent to L-ascorbic acid[a]	% Change of phosphorescence intensity
NAC-Mn/ZnS	Na^+	5000	1.3
	K^+	5000	0.8
	Mg^{2+}	5000	1.2
	Ca^{2+}	5000	0.9
	L-cysteine	500	1
	Histidine	500	0.7
	Tryptophan	500	1.2
	Glucose	500	1.4
	BSA	50	−5
Cys-Mn/ZnS	Na^+	5000	1.2
	K^+	5000	0.9
	Mg^{2+}	5000	1.1
	Ca^{2+}	5000	0.8
	L-cysteine	500	1
	Histidine	500	0.8
	Tryptophan	500	1.2
	Glucose	500	1.5
	BSA	50	−4.3

[a] Concentration of L-ascorbic acid is 5.0 μM.

Table 2
Recovery test of L-ascorbic acid in real urine samples using the proposed and reference method.

Found[a] (μM)					Recovery (%)		
Sample	Added (μM)	NAC-Mn/ZnS QDs method	Cys-Mn/ZnS QDs method	Reference method	NAC-Mn/ZnS QDs method	Cys-Mn/ZnS QDs method	Reference method
1	0.0	ND[b]	ND[b]	ND[b]	–	–	–
2	25.0	24.7 ± 0.07	25.0 ± 0.07	25.08 ± 0.06	98.8	100	100
3	35.0	34.3 ± 0.08	34.1 ± 0.10	35.9 ± 0.08	97.9	97.2	102

[a] $n=3$.
[b] ND: Not detected.

Table 3
Comparison of analytical features of the present method with some other methods for the determination of L-ascorbic acid.

Method	Linear range (μM)	Detection limit (μM)	[Ref.]
Voltammetry	6.0–800.0	0.523	[8]
HPLC	41.0–69.0	0.284	[13]
Ultraviolet spectrophotometry	11.0–280.0	7.39	[5]
Kinetic-fluorimetric method	57–680.0	0.0909	[6]
Enzymatic method	0.10–1.0	0.102	[7]
Colorimetric probe	0.044–0.3	0.00301	[9]
Non-aggregation colorimetric sensor	0.1–2.5	0.0489	[10]
Aggregation colorimetric sensor	0.11–85.0	0.0199	[11]
Chemiluminescence based on QDs	0.10–100.0	0.0067	[12]
Phosphorescence using NAC-Mn/ZnS QDs	2.5–37.5	0.72	This work
Phosphorescence using Cys-Mn/ZnS QDs	2.5–47.5	1.38	This work

Mn/ZnS QDs and thus causing the phosphorescence quenching [40–42]. In addition, since AA behaves as a vinyl carboxylic acid, its double bond will transmit electron pairs between the hydroxyl and carbonyl moieties. AA is most likely to degrade into oxalic acid under basic conditions which can also induce phosphorescence quenching of Mn/ZnS QDs [29].

3.5. Interference of co-existing foreign substances

To evaluate the selectivity of Mn/ZnS QDs for detecting AA, the phosphorescence intensities of Mn/ZnS QDs to the potential interferents in urine fluid are assessed. Here, the concentration of AA is 5.0 μM. Table 1 summarizes the % change of the phosphorescence intensity of Mn/ZnS QDs in the presence of interferents. The intensities are unaffected by 5000-fold excess of Na^+, Mg^{2+}, K^+, and Ca^{2+}. Amino acids such as L-cysteine, histidine and tryptophan at 500-fold concentration of AA also show no interference with the detection of AA. Glucose does not affect the detection at a 500-fold concentration of AA. Only 50-fold excess of BSA causes a slightly interference. These results demonstrate that our proposed method can be applied to determine AA in urine sample.

3.6. Determination of AA in urine sample

It has been reported that biological fluids demonstrate significant auto-fluorescent background but insignificant RTP background [28]. The remarkable advantages of the RTP made it promising for the analysis of biological fluids. To investigate the possibility of real application, our proposed method is applied to determine AA in urine. Table 2 summarizes the recovery tests of AA in urine samples obtained by the proposed and reference method [5]. The recovery is 97.2–102% and the results obtained by both methods are in consistent, demonstrating that the potential of our as-synthesized Mn/ZnS QDs for detection of AA in urine samples.

4. Conclusion

In this work, water-soluble NAC-Mn/ZnS QDs and Cys-Mn/ZnS QDs have been synthesized which possess excellent phosphorescent properties. These Mn/ZnS QDs are efficiently quenched by AA and show high selectivity to AA. The results obtained by the present method are in complete agreement with that of the reference method, demonstrating that it can be potentially useful for determination of AA in urine samples. The Stern–Volmer plot and phosphorescence decay of Mn/ZnS QDs indicate the dynamic quenching mechanism. In addition, NAC-Mn/ZnS QDs displays higher sensitivity and lower LOD than that of Cys-Mn/ZnS QDs for detection of AA. Comparing with other methods for AA detection (Table 3), the present method exhibits better characteristics in terms of long luminescence lifetime, simple sample preparation procedure, immune to interference from oxygen, fluorescence and scattering in biological system, excellent biocompatibility and low toxicity in biological fluids, although the sensitivity is not higher than some other methods. It is anticipated that Mn/ZnS QDs can also be a promising luminescent material for fabrication of novel phosphorescence nano-probes in biological systems.

Acknowledgments

This work is supported by the Hundred Talent Program of Shanxi Province, National Natural Science Foundation of China (21175086 and 21175087), Local Colleges in 2012 National College Students' Innovative Entrepreneurial Training Program (201210114001), Shanxi College Students' Innovative Fund (2012103 and 2013123), Shanxi Medical University Students' Innovation Fund (201231), and 331 Early Career Researcher Grant of Shanxi Medical University Medical School Foundation.

Appendix A. Supplementary material

Supplementary data associated with this article can be found in the online version at http://dx.doi.org/10.1016/j.talanta.2013.07.076.

References

[1] M. Castro, T. Caprile, A. Astuya, C. Millan, K. Reinicke, J.C. Vera, O. Vasquez, L.G. Aguayo, F. Nualart, J. Neurochem. 78 (2001) 815–823.
[2] P. Janda, J. Weber, L. Dunsch, A.B.P. Lever, Anal. Chem. 68 (1996) 960–965.
[3] O. Arrigori, C.D. Tullio, Biochim. Biophys. Acta 1569 (2002) 1–9.
[4] L.K. Massey, M. Liebman, S.A. Kynast-Gales, J. Nutr. 135 (2005) 1673–1677.
[5] H.F. Zhang, L. Zhang, X.H. Yang, Chin. J. Spectrosc. Lab. 26 (2009) 1508–1512.
[6] H.L. Jia, K. Ren, Chin. J. Spectrosc. Lab. 28 (2011) 1702–1705.
[7] T.N. Shekhovtsova, S.V. Muginova, J.A. Luchinina, A.Z. Galimova, Anal. Chim. Acta 573-574 (2006) 125–132.
[8] S. Yilmaz, M. Sadikoglu, G. Saglikoglu, S. Yagmur, G. Askin, J. Electrochem., Science 3 (2008) 1534–1542.
[9] Y.F. Zhang, B.X. Li, C.L. Xu, Analyst 135 (2010) 1579–1584.
[10] G.Q. Wang, Z.P. Chen, L.X. Chen, Nanoscale 3 (2011) 1756–1759.
[11] X.X. Wang, J.M. Liu, S.L. Jiang, L. Jiao, L.P. Lin, M.L. Cui, X.Y. Zhang, L.H. Zhang, Z.Y. Zheng, Sens. Actuators B 182 (2013) 205–210.
[12] H. Chen, R.B. Li, L. Lin, G.S. Guo, J.M. Lin, Talanta 81 (2010) 1688–1696.
[13] Y.J. Pang, J. Chen, C.Y. Cao, Q. Zhang, Mod. J. Integr. Tradit. Chin. West. Med. 18 (2009) 555–556.
[14] M.H. Pournaghi-Azar, H. Razmi-Nerbin, B. Hafezi, Electroanalysis 14 (2002) 206–212.
[15] Y.S. Xia, C.Q. Zhu, Microchim. Acta 164 (2009) 29–34.
[16] W.J. Jin, M.T. Fernández-Argüelles, J.M. Costa-Fernández, R. Pereiro, A. Sanz-Medel, Chem. Commun. (2005) 883–885.
[17] D.B. Cordes, S. Gamsey, B. Singaram, Angew. Chem. Int. Ed. 45 (2006) 3832–3829.
[18] L.Y. Wang, L. Wang, F. Gao, Z.Y. Yu, Z.M. Wu, Analyst 127 (2002) 977–980.
[19] H.Q. Yao, Y. Zhang, F. Xiao, Z.Y. Xia, J.H. Rao, Angew. Chem. Int. Ed. 46 (2007) 4346–4349.
[20] J. Kuijt, F. Ariese, U.A.T. Brinkman, C. Gooijer, Anal. Chim. Acta 488 (2003) 135–171.
[21] I. Sánchez-Barragaán, J.M. Costa-Fernández, M. Valledor, J.C. Campo, A. Sanz-Medel, Trends Anal. Chem. 25 (2006) 958–967.
[22] J.M. Traviesa-Alvarez, I. Sánchez-Barragan, J.M. Costa-Fernández, R. Pereiro, A. Sauz-Medel, Analyst 132 (2007) 218–223.
[23] N. Pradhan, D. Goorskey, J. Thessing, X.G. Peng, J. Am. Chem. Soc. 127 (2005) 17586–17587.
[24] D.J. Norris, A.L. Efros, S.C. Erwin, Science 319 (2008) 1776–1779.
[25] Y. He, X.P. Yan, Sci. China Chem. 54 (2011) 1254–1259.
[26] H.F. Wang, Y. He, T.R. Ji, X.P. Yan, Anal. Chem. 81 (2009) 1615–1621.
[27] P. Wu, Y. He, H.F. Wang, X.P. Yan, Anal. Chem. 82 (2010) 1427–1433.
[28] Y. He, H.F. Wang, X.P. Yan, Anal. Chem. 80 (2008) 3832–3837.
[29] H.F. Wang, Y. Li, Y.Y. Wu, Y. He, X.P. Yan, Chem. Eur. J. 16 (2010) 12988–12994.
[30] H. Wu, Z.F. Fan, Spectrochim. Acta A 90 (2012) 131–134.
[31] J.Q. Zhuang, X.D. Zhang, G. Wang, D.M. Li, W.S. Yang, T.J. Li, J. Mater. Chem. 13 (2003) 1853–1857.
[32] J.H. Chung, C.S. Ah, D.J. Jang, J. Phys. Chem. B 105 (2001) 4128–4132.
[33] J.R. Lakowicz, Principles of Fluorescence Spectroscopy, Kluwer Academic/Plenum Press, New York (1999) 1–698.
[34] B. Valeur, Molecular Fluorescence: Principles and Applications, Wiley-VCH, Weinheim (2001) 72–86.
[35] Y. He, H.-F. Wang, X.-P. Yan, Anal. Chem. 80 (2008) 3832–3837.
[36] J.F. Suyver, S.F. Wuister, J.J. Kelly, A. Meijerink, Nano Lett. 1 (2001) 429–433.
[37] H. Yang, S. Santra, P.H. Holloway, J. Nanosci. Nanotechnol. 5 (2005) 1364–1375.
[38] Y. He, H.-F. Wang, X.-P. Yan, Chem. Eur. J 15 (2009) 5436–5440.
[39] Y. Ma, C. Yang, N. Li, Y.-R. Yang, Talanta 67 (2005) 979–983.
[40] S. Jagadeeswari, M.A. Jhonsi, A. Kathiravan, R. Renganathan, J. Lumin. 131 (2011) 597–602.
[41] S. Ghosh, S.C. Bhattacharya, A. Saha, Anal. Bioanal. Chem. 397 (2010) 1573–1582.
[42] Z.Q. Liu, P.-F. Yin, P.P. Li, X.D. Wang, Y.Q. He, J. Lumin. 132 (2012) 2484–2488.